



Fermi National Accelerator Laboratory

FERMILAB-Conf-95/217-E

D0

**Measurement of Inclusive Triple Differential Dijet Cross Section,
 $d^3\sigma/dE_T d\eta_1 d\eta_2$ in $p\bar{p}$ Collisions at $\sqrt{s} = 1.8$ TeV**

S. Abachi et al.

The D0 Collaboration

*Fermi National Accelerator Laboratory
P.O. Box 500, Batavia, Illinois 60510*

July 1995

Submitted to the *International Europhysics Conference on High Energy Physics (HEP 95)*,
Brussels, Belgium, July 27-August 2, 1995

Disclaimer

This report was prepared as an account of work sponsored by an agency of the United States Government. Neither the United States Government nor any agency thereof, nor any of their employees, makes any warranty, expressed or implied, or assumes any legal liability or responsibility for the accuracy, completeness, or usefulness of any information, apparatus, product, or process disclosed, or represents that its use would not infringe privately owned rights. Reference herein to any specific commercial product, process, or service by trade name, trademark, manufacturer, or otherwise, does not necessarily constitute or imply its endorsement, recommendation, or favoring by the United States Government or any agency thereof. The views and opinions of authors expressed herein do not necessarily state or reflect those of the United States Government or any agency thereof.

Measurement of the Inclusive Triple Differential Dijet Cross Section, $d^3\sigma/dE_T d\eta_1 d\eta_2$ in $p\bar{p}$ Collisions at $\sqrt{s} = 1.8$ TeV

The DØ Collaboration¹
(July 1995)

Measurement of the inclusive triple differential dijet cross section, $d^3\sigma/dE_T d\eta_1 d\eta_2$, is described. This cross section was measured at the Fermilab Tevatron $p\bar{p}$ collider at a center of mass energy $\sqrt{s} = 1.8$ TeV with the DØ detector during the 1992-1993 run. The sensitivity of this measurement to different parton distribution functions is explored. A comparison of the data to NLO theory using different parton distributions functions indicates the need for a smaller gluon content in the x range accessible at the Tevatron than is predicted by current parton distribution sets.

S. Abachi,¹² B. Abbott,³⁴ M. Abolins,²³ B.S. Acharya,⁴¹ I. Adam,¹⁰ D.L. Adams,³⁵ M. Adams,¹⁵
S. Ahn,¹² H. Aihara,²⁰ J. Alitti,³⁷ G. Álvarez,¹⁶ G.A. Alves,⁸ E. Amidi,²⁷ N. Amos,²²
E.W. Anderson,¹⁷ S.H. Aronson,³ R. Astur,³⁹ R.E. Avery,²⁹ A. Baden,²¹ V. Balamurali,³⁰
J. Balderston,¹⁴ B. Baldin,¹² J. Bantly,⁴ J.F. Bartlett,¹² K. Bazizi,⁷ J. Bendich,²⁰ S.B. Beri,³²
I. Bertram,³⁵ V.A. Bezzubov,³³ P.C. Bhat,¹² V. Bhatnagar,³² M. Bhattacharjee,¹¹ A. Bischoff,⁷
N. Biswas,³⁰ G. Blazey,¹² S. Blessing,¹³ P. Bloom,⁵ A. Boehnlein,¹² N.I. Bojko,³³
F. Borchering,¹² J. Borders,³⁶ C. Boswell,⁷ A. Brandt,¹² R. Brock,²³ A. Bross,¹² D. Buchholz,²⁹
V.S. Burtovoi,³³ J.M. Butler,¹² D. Casey,³⁶ H. Castilla-Valdez,⁹ D. Chakraborty,³⁹
S.-M. Chang,²⁷ S.V. Chekulaev,³³ L.-P. Chen,²⁰ W. Chen,³⁹ L. Chevalier,³⁷ S. Chopra,³²
B.C. Choudhary,⁷ J.H. Christenson,¹² M. Chung,¹⁵ D. Claes,³⁹ A.R. Clark,²⁰ W.G. Cobau,²¹
J. Cochran,⁷ W.E. Cooper,¹² C. Cretsinger,³⁶ D. Cullen-Vidal,⁴ M.A.C. Cummings,¹⁴ D. Cutts,⁴
O.I. Dahl,²⁰ K. De,⁴² M. Demarteau,¹² R. Demina,²⁷ K. Denisenko,¹² N. Denisenko,¹²
D. Denisov,¹² S.P. Denisov,³³ W. Dharmaratna,¹³ H.T. Diehl,¹² M. Diesburg,¹² G. Di Loreto,²³
R. Dixon,¹² P. Draper,⁴² J. Drinkard,⁶ Y. Ducros,³⁷ S.R. Dugad,⁴¹ S. Durston-Johnson,³⁶
D. Edmunds,²³ J. Ellison,⁷ V.D. Elvira,^{12,†} R. Engelmann,³⁹ S. Eno,²¹ G. Eppley,³⁵
P. Ermolov,²⁴ O.V. Eroshin,³³ V.N. Evdokimov,³³ S. Fahey,²³ T. Fahland,⁴ M. Fatyga,³
M.K. Fatyga,³⁶ J. Featherly,³ S. Feher,³⁹ D. Fein,² T. Ferbel,³⁶ G. Finocchiaro,³⁹ H.E. Fisk,¹²
Yu. Fisysak,²⁴ E. Flattum,²³ G.E. Forden,² M. Fortner,²⁸ K.C. Frame,²³ P. Franzini,¹⁰ S. Fuess,¹²
A.N. Galjaev,³³ E. Gallas,⁴² C.S. Gao,^{12,*} S. Gao,^{12,*} T.L. Geld,²³ R.J. Genik II,²³ K. Genser,¹²
C.E. Gerber,^{12,§} B. Gibbard,³ V. Glebov,³⁶ S. Glenn,⁵ B. Gobbi,²⁹ M. Goforth,¹³
A. Goldschmidt,²⁰ B. Gómez,¹ P.I. Goncharov,³³ H. Gordon,³ L.T. Goss,⁴³ N. Graf,³
P.D. Grannis,³⁹ D.R. Green,¹² J. Green,²⁸ H. Greenlee,¹² G. Griffin,⁶ N. Grossman,¹²
P. Grudberg,²⁰ S. Grünendahl,³⁶ W. Gu,^{12,*} G. Guglielmo,³¹ J.A. Guida,³⁹ J.M. Guida,³
W. Gurny,³ S.N. Gurzhiev,³³ P. Gutierrez,³¹ Y.E. Gutnikov,³³ N.J. Hadley,²¹ H. Haggerty,¹²
S. Hagopian,¹³ V. Hagopian,¹³ K.S. Hahn,³⁶ R.E. Hall,⁶ S. Hansen,¹² R. Hatcher,²³
J.M. Hauptman,¹⁷ D. Hedin,²⁸ A.P. Heinson,⁷ U. Heintz,¹² R. Hernández-Montoya,⁹
T. Heuring,¹³ R. Hirosky,¹³ J.D. Hobbs,¹² B. Hoeneisen,^{1,¶} J.S. Hoftun,⁴ F. Hsieh,²² Ting Hu,³⁹
Tong Hu,¹⁶ T. Huehn,⁷ S. Igarashi,¹² A.S. Ito,¹² E. James,² J. Jaques,³⁰ S.A. Jerger,²³

¹ Submitted to the XVII International Symposium on Lepton-Photon Interactions (LP95), Beijing, China, August 10-15, 1995.

J.Z.-Y. Jiang,³⁹ T. Joffe-Minor,²⁹ H. Johari,²⁷ K. Johns,² M. Johnson,¹² H. Johnstad,⁴⁰
A. Jonckheere,¹² M. Jones,¹⁴ H. Jöstlein,¹² S.Y. Jun,²⁹ C.K. Jung,³⁹ S. Kahn,³ G. Kalbfleisch,³¹
J.S. Kang,¹⁸ R. Kehoe,³⁰ M.L. Kelly,³⁰ A. Kernan,⁷ L. Kerth,²⁰ C.L. Kim,¹⁸ S.K. Kim,³⁸
A. Klatchko,¹³ B. Klima,¹² B.I. Klochkov,³³ C. Klopfenstein,³⁹ V.I. Klyukhin,³³
V.I. Kochetkov,³³ J.M. Kohli,³² D. Koltick,³⁴ A.V. Kostritskiy,³³ J. Kotcher,³ J. Kourlas,²⁶
A.V. Kozelov,³³ E.A. Kozlovski,³³ M.R. Krishnaswamy,⁴¹ S. Krzywdzinski,¹² S. Kunori,²¹
S. Lami,³⁹ G. Landsberg,¹² R.E. Lanou,⁴ J-F. Lebrat,³⁷ A. Leflat,²⁴ H. Li,³⁹ J. Li,⁴² Y.K. Li,²⁹
Q.Z. Li-Demarteau,¹² J.G.R. Lima,⁸ D. Lincoln,²² S.L. Linn,¹³ J. Linnemann,²³ R. Lipton,¹²
Y.C. Liu,²⁹ F. Lobkowicz,³⁶ S.C. Loken,²⁰ S. Lökös,³⁹ L. Lueking,¹² A.L. Lyon,²¹
A.K.A. Maciel,⁸ R.J. Madaras,²⁰ R. Madden,¹³ I.V. Mandrichenko,³³ Ph. Mangeot,³⁷ S. Mani,⁵
B. Mansoulié,³⁷ H.S. Mao,^{12,*} S. Margulies,¹⁵ R. Markeloff,²⁸ L. Markosky,² T. Marshall,¹⁶
M.I. Martin,¹² M. Marx,³⁹ B. May,²⁹ A.A. Mayorov,³³ R. McCarthy,³⁹ T. McKibben,¹⁵
J. McKinley,²³ T. McMahon,³¹ H.L. Melanson,¹² J.R.T. de Mello Neto,⁸ K.W. Merritt,¹²
H. Miettinen,³⁵ A. Milder,² A. Mincer,²⁶ J.M. de Miranda,⁸ C.S. Mishra,¹²
M. Mohammadi-Baarmand,³⁹ N. Mokhov,¹² N.K. Mondal,⁴¹ H.E. Montgomery,¹² P. Mooney,¹
M. Mudan,²⁶ C. Murphy,¹⁶ C.T. Murphy,¹² F. Nang,⁴ M. Narain,¹² V.S. Narasimham,⁴¹
A. Narayanan,² H.A. Neal,²² J.P. Negret,¹ E. Neis,²² P. Nemethy,²⁶ D. Nešić,⁴ D. Norman,⁴³
L. Oesch,²² V. Oguri,⁸ E. Oltman,²⁰ N. Oshima,¹² D. Owen,²³ P. Padley,³⁵ M. Pang,¹⁷ A. Para,¹²
C.H. Park,¹² Y.M. Park,¹⁹ R. Partridge,⁴ N. Parua,⁴¹ M. Paterno,³⁶ J. Perkins,⁴² A. Peryshkin,¹²
M. Peters,¹⁴ H. Piekarz,¹³ Y. Pischalnikov,³⁴ A. Pluquet,³⁷ V.M. Podstavkov,³³ B.G. Pope,²³
H.B. Prosper,¹³ S. Protopopescu,³ D. Pušeljčić,²⁰ J. Qian,²² P.Z. Quintas,¹² R. Raja,¹²
S. Rajagopalan,³⁹ O. Ramirez,¹⁵ M.V.S. Rao,⁴¹ P.A. Rapidis,¹² L. Rasmussen,³⁹ A.L. Read,¹²
S. Reucroft,²⁷ M. Rijssenbeek,³⁹ T. Rockwell,²³ N.A. Roe,²⁰ P. Rubinov,³⁹ R. Ruchti,³⁰
S. Rusin,²⁴ J. Rutherford,² A. Santoro,⁸ L. Sawyer,⁴² R.D. Schamberger,³⁹ H. Schellman,²⁹
J. Sculli,²⁶ E. Shabalina,²⁴ C. Shaffer,¹³ H.C. Shankar,⁴¹ R.K. Shivpuri,¹¹ M. Shupe,²
J.B. Singh,³² V. Sirotenko,²⁸ W. Smart,¹² A. Smith,² R.P. Smith,¹² R. Snihur,²⁹ G.R. Snow,²⁵
S. Snyder,³⁹ J. Solomon,¹⁵ P.M. Sood,³² M. Sosebee,⁴² M. Souza,⁸ A.L. Spadafora,²⁰
R.W. Stephens,⁴² M.L. Stevenson,²⁰ D. Stewart,²² D.A. Stoianova,³³ D. Stoker,⁶ K. Streets,²⁶
M. Strovink,²⁰ A. Taketani,¹² P. Tamburello,²¹ J. Tarazi,⁶ M. Tartaglia,¹² T.L. Taylor,²⁹
J. Teiger,³⁷ J. Thompson,²¹ T.G. Trippe,²⁰ P.M. Tuts,¹⁰ N. Varelas,²³ E.W. Varnes,²⁰
P.R.G. Virador,²⁰ D. Vititoe,² A.A. Volkov,³³ A.P. Vorobiev,³³ H.D. Wahl,¹³ G. Wang,¹³
J. Wang,^{12,*} L.Z. Wang,^{12,*} J. Warchol,³⁰ M. Wayne,³⁰ H. Weerts,²³ F. Wen,¹³ W.A. Wenzel,²⁰
A. White,⁴² J.T. White,⁴³ J.A. Wightman,¹⁷ J. Wilcox,²⁷ S. Willis,²⁸ S.J. Wimpenny,⁷
J.V.D. Wirjawan,⁴³ J. Womersley,¹² E. Won,³⁶ D.R. Wood,¹² H. Xu,⁴ R. Yamada,¹² P. Yamin,³
C. Yanagisawa,³⁹ J. Yang,²⁶ T. Yasuda,²⁷ C. Yoshikawa,¹⁴ S. Youssef,¹³ J. Yu,³⁶ Y. Yu,³⁸
Y. Zhang,^{12,*} Y.H. Zhou,^{12,*} Q. Zhu,²⁶ Y.S. Zhu,^{12,*} Z.H. Zhu,³⁶ D. Zieminska,¹⁶ A. Zieminski,¹⁶
and A. Zylberstejn³⁷

¹ Universidad de los Andes, Bogotá, Colombia

² University of Arizona, Tucson, Arizona 85721

³ Brookhaven National Laboratory, Upton, New York 11973

⁴ Brown University, Providence, Rhode Island 02912

⁵ University of California, Davis, California 95616

⁶ University of California, Irvine, California 92717

⁷ University of California, Riverside, California 92521

⁸ LAFEX, Centro Brasileiro de Pesquisas Físicas, Rio de Janeiro, Brazil

⁹ CINVESTAV, Mexico City, Mexico

¹⁰ Columbia University, New York, New York 10027

¹¹ Delhi University, Delhi, India 110007

¹² Fermi National Accelerator Laboratory, Batavia, Illinois 60510

¹³ Florida State University, Tallahassee, Florida 32306

- ¹⁴University of Hawaii, Honolulu, Hawaii 96822
¹⁵University of Illinois at Chicago, Chicago, Illinois 60607
¹⁶Indiana University, Bloomington, Indiana 47405
¹⁷Iowa State University, Ames, Iowa 50011
¹⁸Korea University, Seoul, Korea
¹⁹Kyungshung University, Pusan, Korea
²⁰Lawrence Berkeley Laboratory and University of California, Berkeley, California 94720
²¹University of Maryland, College Park, Maryland 20742
²²University of Michigan, Ann Arbor, Michigan 48109
²³Michigan State University, East Lansing, Michigan 48824
²⁴Moscow State University, Moscow, Russia
²⁵University of Nebraska, Lincoln, Nebraska 68588
²⁶New York University, New York, New York 10003
²⁷Northeastern University, Boston, Massachusetts 02115
²⁸Northern Illinois University, DeKalb, Illinois 60115
²⁹Northwestern University, Evanston, Illinois 60208
³⁰University of Notre Dame, Notre Dame, Indiana 46556
³¹University of Oklahoma, Norman, Oklahoma 73019
³²University of Panjab, Chandigarh 16-00-14, India
³³Institute for High Energy Physics, 142-284 Protvino, Russia
³⁴Purdue University, West Lafayette, Indiana 47907
³⁵Rice University, Houston, Texas 77251
³⁶University of Rochester, Rochester, New York 14627
³⁷CEA, DAPNIA/Service de Physique des Particules, CE-SACLAY, France
³⁸Seoul National University, Seoul, Korea
³⁹State University of New York, Stony Brook, New York 11794
⁴⁰SSC Laboratory, Dallas, Texas 75237
⁴¹Tata Institute of Fundamental Research, Colaba, Bombay 400005, India
⁴²University of Texas, Arlington, Texas 76019
⁴³Texas A&M University, College Station, Texas 77843

INTRODUCTION

Recent theoretical and experimental advances in high energy physics are making it possible to explore a wide range of issues in perturbative Quantum Chromodynamics (pQCD). Experimentally, higher energies, high luminosity, and improved detectors are allowing us to examine regions in phase space where leading order (LO) predictions are not enough to fully explain measured results. Next-to-leading order ($\mathcal{O}(\alpha_s^3)$) pQCD (NLO) and mixed scale predictions have recently become available (1-4). Jet production at the Tevatron, dominated by gluon-gluon scattering, should provide new constraints on the small x distribution functions.

In the parton model, the hard scattering process in a $p\bar{p}$ collision takes place when a parton in the proton collides with a parton in the anti-proton. The dijet cross section is a convolution of the parton distribution functions (pdf's), $f(x, Q^2)$, and the parton-parton subprocess, $\hat{\sigma}$:

$$\frac{d^3\sigma}{dE_T d\eta_1 d\eta_2} \sim \sum_{i,j} f_i(x_1, Q^2) f_j(x_2, Q^2) \hat{\sigma}_{ij}(E_T, \eta_1, \eta_2) \quad (1)$$

where $x_{1(2)}$ is the momentum fraction of the proton (anti-proton) carried by the colliding parton; $f_{i,j}$ are the parton distribution functions, evaluated at the energy scale of the hard

scattering, Q^2 ; E_T is the transverse energy; and η_1 and η_2 are the pseudorapidities of the outgoing partons. The momentum fractions, x_1 and x_2 , of the incoming partons can be written in terms of the pseudorapidities of the final state partons (for massless partons):

$$x_{1,2} = \frac{1}{\sqrt{s}} \sum_i^N E_{Ti} e^{(\pm\eta_i)} \quad (2)$$

where $N = 2, 3$ is the number of jets, depending on the order of the theoretical calculation (LO or NLO) and 1, 2 correspond to summing over negative or positive η_i .

NLO theory has proven to be successful in describing jet production in hadronic collisions (e.g., (5,6)). To the extent that NLO provides an adequate description of jet production, the dijet cross sections will provide information on the pdf's. For $E_T \sim 45$ GeV and $\eta_1 = \eta_2 = 0.0$, x_1 and x_2 are ~ 0.05 . On the other hand, for $\eta_1 = \eta_2 = 3.0$, the x -values are ~ 0.002 and ~ 0.98 . Thus the ability to measure high rapidity final states is necessary to reach the very small and very large x regions of phase space. At very low- x , gluons dominate, hence the dijet cross section is sensitive to the gluon distribution functions.

Theoretically, next-to-leading order predictions have several advantages over the leading order prediction, in particular, a decreased sensitivity to the renormalization scale, μ . However, in NLO, the additional radiated gluon creates a dependence on the jet algorithm used to reconstruct jets. This analysis takes advantage of a new NLO parton level event generator, JETRAD (1), a full NLO tree level plus one loop calculation. JETRAD provides the flexibility to choose the order of the calculation (LO or NLO); the renormalization scale; the input pdf; the E_T and η range for inclusive or exclusive jet production; and the jet algorithm. We exploit these features within JETRAD in conjunction with our data to test the theoretical predictions of NLO with different input parton distribution functions.

There are several theoretical groups which produce sets of pdf's, including the CTEQ (7), MRS (3), and GRV (8) collaborations. The different pdf sets can be based on different input data (as newer data becomes available, new pdf's are generated by the various groups) or on different input assumptions such as requiring a more or less singular gluon distribution. There will be several parton distribution functions used in this analysis. CTEQ2M is the current best fit pdf from the CTEQ collaboration, allowing Λ_{QCD} to float to a best value and using NLO theory to derive the pdf's. Likewise, MRSD-' and GRV are best fit pdf's from MRS and GRV. CTEQ2MS assumes a more singular gluon pdf while CTEQ2MF and MRSD'_0 assume less singular gluon pdf's. CTEQ2ML assumes a high value of Λ_{QCD} .

DETECTOR

The DØ detector (9) is a general purpose particle physics detector with excellent calorimetric energy and spatial resolution, and a high degree of hermeticity. The analysis described here utilizes mainly the calorimetry. The calorimeter uses liquid argon to sample the energy of particle showers which result from $p\bar{p}$ collisions. Its coverage extends to $|\eta| \leq 4.0$. The calorimeters have electromagnetic and hadronic resolutions of $15\%/\sqrt{E}$ and $50\%/\sqrt{E}$, respectively. Jet resolution is typically $80\%/\sqrt{E}$. During the 1992-1993 data taking run, the jet triggers were implemented to $|\eta| \leq 3.2$.

DATA ANALYSIS

The inclusive differential dijet cross section is given by:

$$\frac{d^3\sigma}{dE_T d\eta_1 d\eta_2} = \frac{N_{\text{events}}}{\mathcal{L}_{\text{trig}} \epsilon_{\text{event}} \Delta E_T \Delta \eta_1 \Delta \eta_2} \quad (3)$$

where E_T is the energy of the leading (most energetic) jet, η_1 and η_2 are the pseudorapidities of the two leading jets; N_{events} is the number of events observed in the specific ΔE_T , $\Delta \eta_1$, and $\Delta \eta_2$ ranges or bins; $\mathcal{L}_{\text{trig}}$ is the integrated luminosity of the trigger used to collect the data; and ϵ_{event} is the efficiency to collect an event with the specific E_T , η_1 , η_2 topology and includes the trigger efficiency, the jet reconstruction efficiency, the efficiency for both jets to pass the jet quality cuts, and the detector acceptance. In constructing this cross section, events are double counted, *i.e.*, the leading jet enters the cross section as *jet 1* with the second most energetic jet as *jet 2*, and then the second most energetic jet is binned as *jet 1* with the leading jet binned as *jet 2*. This double counting ensures infrared safety for the cross section (1).

In the offline analysis, jets are reconstructed with a fixed cone algorithm of $R = \sqrt{\Delta\eta^2 + \Delta\phi^2} = 0.7$. In order to eliminate fake jets caused by noisy calorimeter cells, cosmic rays, and beam losses, we apply a standard set of jet quality cuts on a jet by jet basis. Jets that fail any of the cuts are removed. At 50 GeV these cuts are more than 97% effective at removing fake jets while removing less than 4% of real jets. We require ≥ 2 jets in an event. The leading two jets of each event in the sample must pass the quality cuts and must satisfy $E_T \geq 20$ GeV. A single interaction is also required. The jet pseudorapidities are corrected for reconstruction biases. Lastly, an energy scale correction is applied to the jet energies. This correction varies from 15 – 25% as a function of E_T and η . This corrects for various detector effects which cause a mismeasurement of the jet energies and is the major source of systematic error in the measurement.

After jet and event selection and applying the above corrections, the cross sections can be calculated according to Equation 3. A threefold differential cross section must be integrated over one or more variables to be viewed. Figure 1 shows the cross section, $d^3\sigma/dE_T d\eta_1 d\eta_2$, integrated over the range $45.0 \leq E_T < 55.0$ GeV as a function of η_1 and η_2 . The cutoffs in η_1 and η_2 are due solely to the kinematic range of the dijet cross section.

We choose to plot the cross section in two dimensions as a function of $\eta_2 \times \text{sign}(\eta_1)$, integrating over E_T and $|\eta_1|$; this is referred to as the “signed η distributions.” The advantage of this distribution is that it emphasizes the difference between those events where both jets are on the same side of the detector (positive abscissa) and those events where the jets are on opposite sides of the detector (negative abscissa). A boosted system with both jets on the same side of the detector can only come from one low- x parton and one high- x parton. Thus this method of plotting displays explicit sensitivity to the parton distribution functions.

Detector resolution can have a significant effect on the measured cross sections. Fluctuations in the jet energies due to detector resolution can cause mismeasurement of jet energies with respect to the original parton jet energies. This introduces the possibility of misordering of jets in E_T . For events with only two jets, this is not a significant problem due to the double counting. However, for events with more than two jets, a misordering in E_T can lead to an event topology very different from the parton level event and significantly affect the cross section measurement. DØ has studied this effect using JETRAD by generating NLO parton events with and without smearing by the detector resolution. These studies have been used to correct the signed η distributions back to the parton jet distributions.

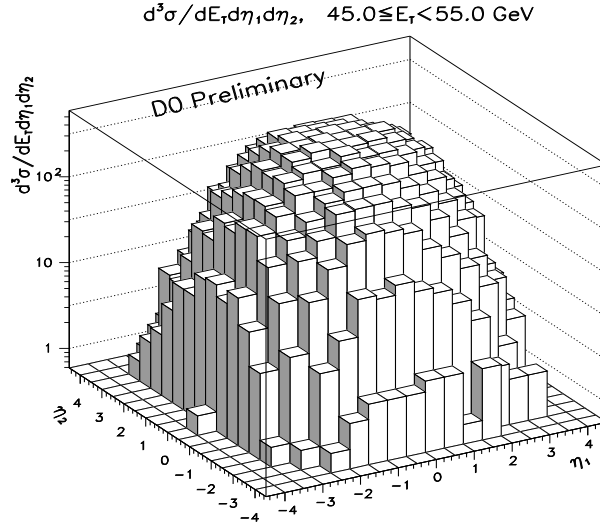


FIG. 1. The inclusive dijet cross section, $d^3\sigma/dE_T d\eta_1 d\eta_2$ as a function of η_1 and η_2 for $45.0 \leq E_T < 55.0$ GeV.

RESULTS

After applying all corrections, including the unsmearing factors, we can compare the measured dijet inclusive cross sections to the parton level theoretical predictions of JETRAD. Figure 2 shows one of the signed η distributions, $d^3\sigma/dE_T d\eta_1 d\eta_2$ as a function of $\eta_2 \times \text{sign}(\eta_1)$ for $1.5 \leq |\eta_1| < 2.0$ and $45.0 \leq E_T < 55.0$ GeV. The error bars indicate the statistical error while the dotted band indicates the error due to the jet energy scale correction. The luminosity error of $\pm 12\%$ is not included. The theoretical curve is a JETRAD NLO prediction using the CTEQ2M pdf set and $\mu = E_T$.

We wish to use the signed η distributions to extract information from the cross sections about the gluon distribution function. However, the data has a significant normalization uncertainty due to the luminosity error in addition to the uncertainty due to the energy scale correction ($\sim \pm 30\%$). The theory also has an uncertainty due to the renormalization scale. This μ scale uncertainty varies from 10% at low η rising to a 30% variation for high η .

We consider a comparison of the shapes of data and theory. A shape comparison is valid only if the shapes of the signed η distributions are independent of the uncertainties for both theory (μ scale) and data (energy scale). This shape independence has been verified to hold for $|\eta| \leq 2.5$, with less than a 3% error for central η 's, varying up to $\sim 15\%$ for $|\eta| = 3.0$.

We do a χ^2 minimization of the differences between data and theory, allowing the theory normalization to float. In doing this comparison, the errors on the data and theory take into account the small dependence of the shape on the energy scale (for the data) and the μ scale (for the theory). We determine the χ^2/dof values for a comparison of the experimental signed η distributions with $|\eta| < 3.0$, with the NLO theoretical prediction using different pdf sets, CTEQ2M, CTEQ2MS, CTEQ2MF, CTEQ2ML, MRSD $_0$, MRSD $_0$ ', GRV. We find that none of these pdf sets give a good fit to the data. This lack of agreement can be understood in the context of Fig. 3 which shows the gluon density, $x \times g(x)$ for $Q = 50$ GeV

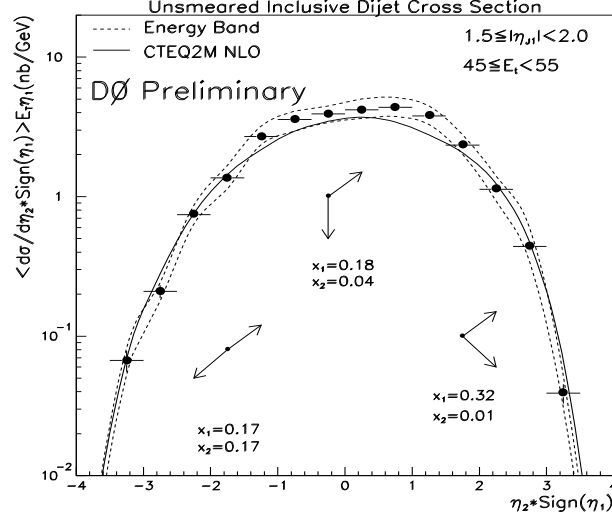


FIG. 2. The inclusive dijet cross section, $d^3\sigma/dE_T d\eta_1 d\eta_2$ as a function of $\eta_2 \times \text{sign}(\eta_1)$ for $1.5 \leq |\eta| < 2.0$. The cartoons indicate the approximate x values being probed at various regions in the plot.

for various CTEQ pdf sets. As can be seen, at very low x , $x \sim 10^{-4}$, the more singular CTEQ2MS is higher than the flatter CTEQ2MF. Also, there are several places where the various pdf's cross over, in particular, $x = 0.1$. Expanding the areas around $x = 0.1$, Fig. 4 shows that for $x < 0.1$, CTEQ2MF is higher than CTEQ2MS and hence predicts more gluons in that x range while Fig. 5 shows that for $x > 0.1$, CTEQ2MF is lower than CTEQ2MS and hence predicts fewer gluons in that x range. The poor agreement between theory and data for all pdf's may be easily understood in the context of mixing a wide range of x values in the comparison.

We therefore divide the data into three sets, based on the median x_1 and x_2 values of each η_1 and $\eta_2 \times \text{sign}(\eta_1)$ point with $|\eta| \leq 3.0$ and $45.0 \leq E_T < 55.0$ GeV: (1) $x_1 < 0.1$, $x_2 < 0.1$; (2) $x_1 > 0.1$, $x_2 > 0.1$; (3) $x_{1(2)} < 0.1$, $x_{2(1)} > 0.1$. For the smaller x case, $x_{1,2} < 0.1$, the data cannot distinguish between the various pdf sets. For the higher x case, $x_{1,2} > 0.1$, the data favors those pdf sets, CTEQ2MF and MRSD'_0, which have a lower gluon content. In the mixed case, none of the pdf sets give a satisfactory fit to the data.

CONCLUSIONS

We have presented preliminary measurements of the inclusive triple differential dijet cross section, $d^3\sigma/dE_T d\eta_1 d\eta_2$ as a function of $\eta_2 \times \text{sign}(\eta_1)$ for $45.0 \leq E_T < 55.0$ GeV. These signed η distributions favor the parton distribution functions CTEQ2MF and MRSD'_0 for $x > 0.1$. No pdf set fits the data well for regions of phase space with $x_{1(2)} > 0.1$ and $x_{2(1)} < 0.1$, while all sets are acceptable for $x < 0.1$. The data indicate a lower gluon content is necessary for $x > 0.1$ than in current pdf sets.

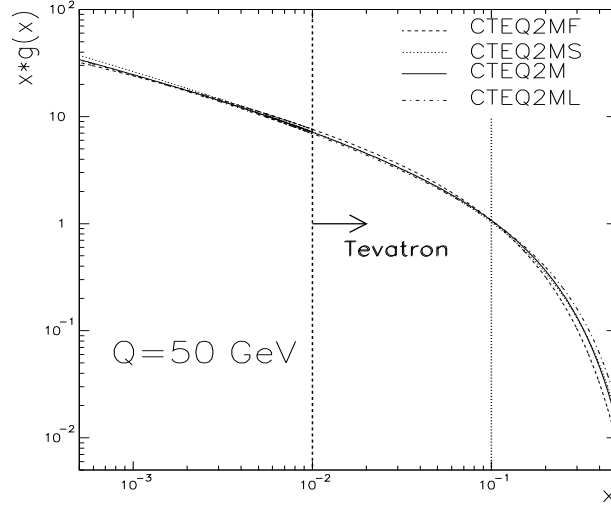


FIG. 3. The gluon distribution as a function of x at $Q=50$ GeV for several pdf's.

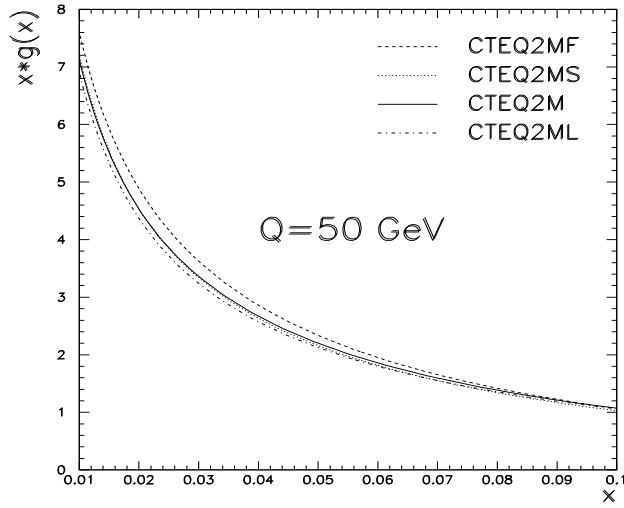


FIG. 4. The gluon distribution as a function of x at $Q=50$ GeV for several pdf's at relatively low x -values.

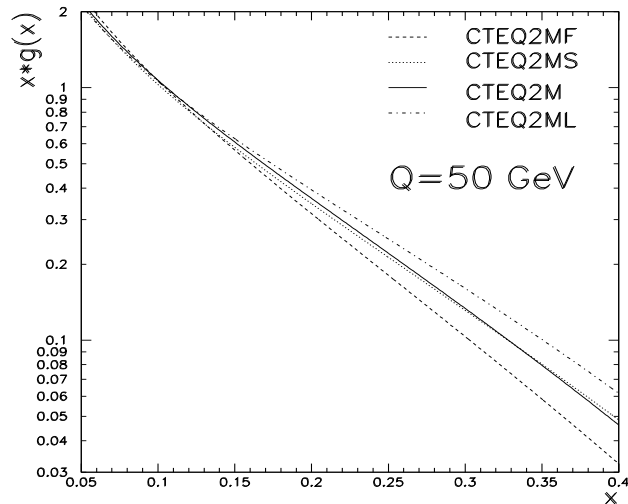


FIG. 5. The gluon distribution as a function of x at $Q=50$ GeV for several pdf's at relatively high x -values.

ACKNOWLEDGEMENTS

We thank the Fermilab Accelerator, Computing, and Research Divisions, and the support staffs at the collaborating institutions for their contributions to the success of this work. We also acknowledge the support of the U.S. Department of Energy, the U.S. National Science Foundation, the Commissariat à L'Energie Atomique in France, the Ministry for Atomic Energy and the Ministry of Science and Technology Policy in Russia, CNPq in Brazil, the Departments of Atomic Energy and Science and Education in India, Colciencias in Colombia, CONACyT in Mexico, the Ministry of Education, Research Foundation and KOSEF in Korea and the A.P. Sloan Foundation.

We are grateful to W. Giele, N. Glover, and D. Kosower for many illuminating theoretical discussions.

REFERENCES

- * Visitor from IHEP, Beijing, China.
 - † Visitor from CONICET, Argentina.
 - § Visitor from Universidad de Buenos Aires, Argentina.
 - ¶ Visitor from Univ. San Francisco de Quito, Ecuador.
1. W.T. Giele, E.W.N. Glover, D.A. Kosower, Fermilab Preprint FERMILAB-Pub-94/070-T (1994).
 2. A.D. Martin, W.J. Stirling, R.G. Roberts, Preprint RAL-93-047 (1993)
 3. A.D. Martin, W.J. Stirling, R.G. Roberts, Phys. Lett. **B306**, 145 (1993); Erratum-*ibid.***B309**, 492 (1993).
 4. V. Del Duca and C.R. Schmidt, Phys. Rev. D **49**, 4510 (1994); preprint **DESY94-114** (1994)
 5. F. Abe *et al.*, (CDF Collaboration), PRL **68**:1104 (1992).
 6. V.D. Elvira (DØ collaboration), Fermilab Preprint FERMILAB-Conf-94/323-E (1994).

7. J. Botts, *et al.*, (CTEQ Collaboration), Phys. Lett. **B304**: 159-166, (1993).
8. M. Gluck, E. Reya, A. Vogt, Z. Phys. **C53**, 127 (1993).
9. S. Abachi *et al.*, (DØ Collaboration), NIM **A338**:185 (1994).